

## Yielding Behavior of Glassy Amorphous Polymers

T. E. Brady and G. S. Y. Yeh

*Department of Chemical and Metallurgical Engineering and The Macromolecular Research Center  
The University of Michigan, Ann Arbor, Michigan 48103*

The effect of thermal history on yielding behavior of atactic polystyrene, isotactic polystyrene, polycarbonate, and polymethyl methacrylate was examined by correlating the deformed microstructure with measured density changes and compressive stress-strain studies. Electron micrographs of bulk polymers and thin films demonstrate the tendency for well-annealed materials to undergo localized shear deformation at 100-1000-Å interspacings, and density measurements show an over-all density increase of about 0.15% upon plastic deformation. Rapid cooling from the melt decreases both the material density (about-0.04%) and the tendency for plastic strain to localize into narrow bands. Compressive stress-strain studies in which the strain rate, test temperature, and thermal history were systematically varied show a semi-logarithmic relationship between nominal strain rate and yield stress. These data were analyzed according to an Eyring-type exponential model where the "shear activation volume" and the "activation energy" were calculated and compared for the ranges of variables studied.

### INTRODUCTION

There is growing evidence for the existence of ordered regions in amorphous polymers. Yeh has carried out high-resolution dark-field microscopy and has reported regions of 15-45 Å in polystyrene<sup>1</sup> and 75 Å in polyethylene terephthalate.<sup>2</sup> Surface textures of about 200 Å have been observed by Carr *et al.*,<sup>3</sup> in polycarbonate while Schoon and Teichmann<sup>4</sup> observed a 50-Å texture in polystyrene and Yang and Kardos<sup>5</sup> reported a 150-Å texture in polysulfone. A recent study by Luch and Yeh<sup>6</sup> revealed a 130-Å texture in thin films of natural rubber using an osmium staining technique.

There is evidence that this texture plays an important role in crystallization of polyethylene terephthalate,<sup>2</sup> polycarbonate,<sup>3</sup> and natural rubber,<sup>6</sup> but generally there is little experimental evidence which defines the nature of this texture and its relation to mechanical properties. One purpose of this study was to identify any correlation between this nonhomogeneous texture of amorphous polymers and yielding behavior, while paying particular attention to the effects of initial thermal history and employing the seldom used compressive geometry.

While numerous stress-strain studies have been reported,<sup>7-12</sup> only recently have Hayward *et al.*<sup>13</sup> and Bowden and Raha<sup>14</sup> studied compressive behavior in detail. The study by Bowden and Raha showed that thermal history, temperature, and strain rate were critical to both the stress-strain relationship and to the tendency for glassy polymers to deform by local shear banding. The onset of localized yielding was predicted by them, using a model previously developed by Bowden.<sup>15</sup>

We have measured the compressive yield stresses

for atactic polystyrene, isotactic polystyrene, polycarbonate, and polymethyl methacrylate while varying temperature, strain rate, and thermal history. The data was analyzed using an Eyring-type exponential model, and the shear activation volume and activation energy were calculated for each set of experimental conditions in an effort to assess the meaning of these parameters with respect to molecular processes.

### EXPERIMENTAL

#### Materials

Shell general purpose atactic polystyrene ( $\bar{M}_w \approx 250\,000$ ), Dow EP 1340-128 isotactic polystyrene ( $\bar{M}_w = 550\,000$ ), Mobay Merlon 60 polycarbonate ( $\bar{M}_w = 38\,000$ ), and Rohm and Haas polymethyl methacrylate cast sheet were used as basic glassy polymer materials in the following experimental studies. Hereafter they will be referred to as APS, IPS, PC, and PMMA, respectively.

#### Electron Microscopy

Thin films (3000-5000 Å thick) of APS and IPS were cast from 0.7% benzene solutions. PC and PMMA thin films were cast from 0.7% methylene chloride solutions. These films were placed on Mylar substrates and heated 15 °C above their respective  $T_g$ 's for 10 min to rid them of solvent and to increase coherency between film and substrate. Each substrate was then drawn 25% at room temperature.

Bulk APS samples were hot stretched 5 : 1 at 130 °C and then water quenched to preserve the orientation required for cold drawing at room temperature. Molded samples of PC and the hot-stretched APS samples were then cold drawn in tension pro-

ducing sharp necks that propagated the lengths of the samples.

APS, IPS, PC, and PMMA samples were compressed in the Instron machine at different rates and different temperatures in order to produce plastic flow in compression. Conventional Pt-C replicas were taken from all the above samples, including the thin films, to study their respective surface textures after plastic deformation.

One additional experiment performed with a PC tensile sample required the deposition of a thin Pt layer upon the surface before deformation.

#### Density Measurements

Densities were measured in gradient columns using an ethylene glycol and water solution for PS and a mixture of NaBr and water for PC and PMMA.<sup>16</sup> Although the measured value of the density appeared to be a function of the residence time in the column (due to absorption), the relative accuracy when comparing two samples placed in the column simultaneously was judged to be better than  $\pm 0.0001 \text{ g/cm}^3$ . Densities were measured as functions of both thermal history and plastic deformation.

#### Mechanical Compression Studies

APS, IPS, PC, and PMMA  $\frac{1}{4}$ -in.-thick sheets were molded and given specific thermal histories by heating above  $T_g$  (above  $T_m$  in the case of crystallizable PC and IPS) and then either ice quenching or slow cooling at  $0.25 \text{ }^\circ\text{C/min}$ , followed by either no subsequent heat treatment or reannealing just below  $T_g$ . Exact thermal histories are listed in Table I. The sheets were cut into  $\frac{1}{2}$  in.  $\times \frac{1}{4}$  in.  $\times \frac{1}{4}$  in. samples, polished, and notched perpendicular to the compression direction to a depth of 0.03 in. using a band-saw file. The notch served as a reproducible defect from which plastic deformation initiated, and the polished surface eliminated other possible deformation sites. Only the PMMA samples were desiccated for 24 h at room temperature and a vacuum of  $10^{-3}$  Torr to eliminate moisture effects. All the polymers with each thermal history were compressed in a circulating air chamber (controllable to  $\pm 0.5 \text{ }^\circ\text{C}$ ) at nominal strain rates of 0.004, 0.04, 0.4, and  $4 \text{ min}^{-1}$  and temperatures ranging from 23 to  $100 \text{ }^\circ\text{C}$ . The ends of the samples were polished but not lubricated.

The yield stress was taken as the peak load divided by the true cross-sectional area at the notch (calculated from Poisson's areal change resulting from a uniaxial strain). The notch and lack of lubrication preclude knowing the absolute yield stress but selected tests comparing several geometries with and without notches and with and with-

TABLE I. Density measurements.

Material	Thermal treatment	Mechanical treatment	Density ( $\text{g/cm}^3$ )
Atactic polystyrene (Shell G. P.)	12 h at $105 \text{ }^\circ\text{C}$ ice quench	none	1.0496
		hot stretch 5:1 at $130 \text{ }^\circ\text{C}$	1.0508
		hot stretch 5:1 at $130 \text{ }^\circ\text{C}$ ; cold drawn (necked) at $25 \text{ }^\circ\text{C}$	1.0519
	12 h at $105 \text{ }^\circ\text{C}$ slow cooled at $0.25 \text{ }^\circ\text{C/min}$	none	1.0497
		cold flow in compression (banded area)	1.0514
		12 h at $105 \text{ }^\circ\text{C}$ ice quench; 6 days at $75 \text{ }^\circ\text{C}$	none
Polymethyl methacrylate (Rohm-Haas cast sheet)	12 h at $105 \text{ }^\circ\text{C}$ slow cooled; 6 days at $75 \text{ }^\circ\text{C}$	none	1.0500
		12 h at $135 \text{ }^\circ\text{C}$ ice quench	1.1900
		hot stretch 5:1 at $130 \text{ }^\circ\text{C}$	1.1915
	12 h at $165 \text{ }^\circ\text{C}$ slow cooled at $0.25 \text{ }^\circ\text{C/min}$	hot stretch 5:1 at $130 \text{ }^\circ\text{C}$ ; cold drawn (necked) at $25 \text{ }^\circ\text{C}$	1.1933
		10 min at $260 \text{ }^\circ\text{C}$ ice quench	1.1938
		1.1960	
Polycarbonate (Mobay M-50)	12 h at $165 \text{ }^\circ\text{C}$ ice quench	none	1.1941
		cold drawn (necked) at $25 \text{ }^\circ\text{C}$	1.1973
		12 h at $165 \text{ }^\circ\text{C}$ slow cooled at $0.25 \text{ }^\circ\text{C/min}$	none
	12 h at $165 \text{ }^\circ\text{C}$ ice quench; 4 days at $145 \text{ }^\circ\text{C}$	none	1.1945
		cold drawn (necked) at $25 \text{ }^\circ\text{C}$	1.1966
		12 h at $165 \text{ }^\circ\text{C}$ slow cooled; 4 days at $145 \text{ }^\circ\text{C}$	none
	cold drawn (necked) at $25 \text{ }^\circ\text{C}$	1.1974	

out lubrication have shown that the functional relationship between nominal strain rate and apparent yield stress is not greatly affected.

The true nominal strain rate was taken as the crosshead velocity divided by the actual sample length at the peak of the load-elongation curve. Again while any nonhomogeneous deformation occurring prior to the peak of the curve precludes knowing the true plastic strain rate, experimentally we have found that the functional relationships between (i) nominal strain rate vs proportional limit stress and (ii) nominal strain rate vs peak stress are nearly identical over the strain-rate range investigated.

## RESULTS

### Electron Microscopy

Figures 1(a) and 1(b) contrast the surface textures of quenched and annealed thin films of APS drawn at

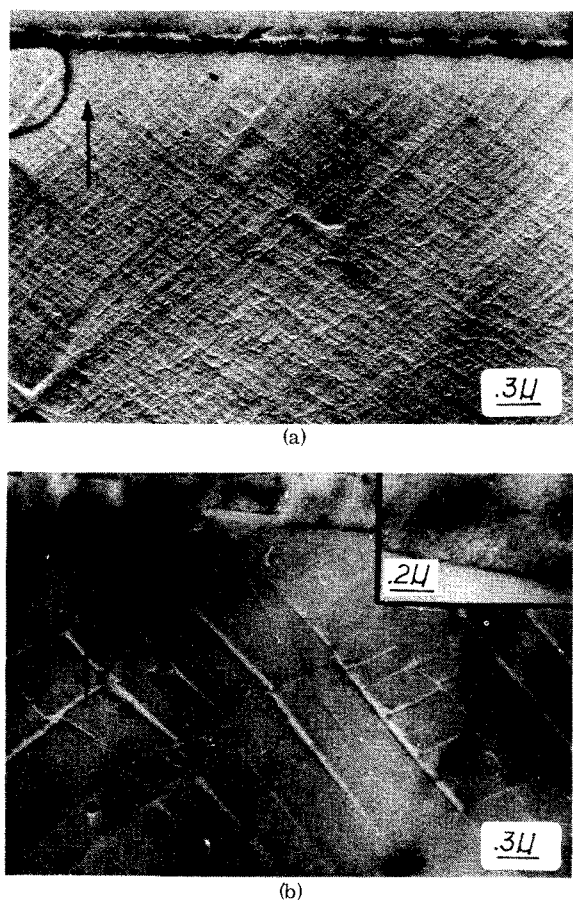


FIG. 1 (a) Pt-C surface replica of atactic polystyrene thin film quenched from 105°C and drawn 25%. 200–400-Å fibrils within the craze are indicated by the small arrows. The vertical arrow in this and subsequent micrographs indicates the strain direction. (b) Pt-C surface replica of atactic polystyrene thin film annealed for 3 days at 75°C and drawn 25%. The small arrow indicates a step formed when a shear band reaches the craze edge. Small arrows in the inset show a 300-Å fibril within the craze.

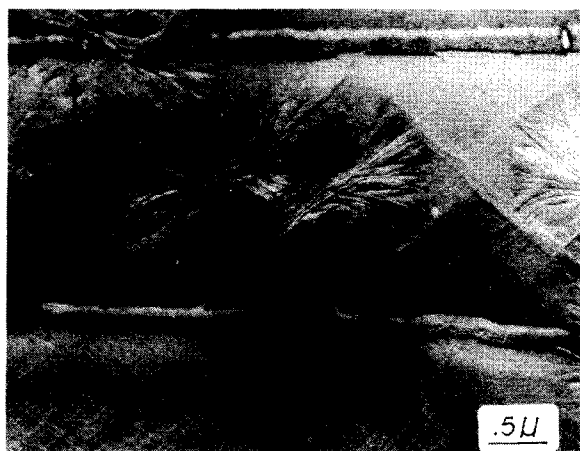
room temperature. Initially crazes develop perpendicular to the stretch direction. Crazing is followed by shear yielding and cold flow clearly evident as discrete shear lines. The crazes consist of fibrillar material  $\sim 300$  Å interspaced by voids of similar dimensions [see inset, Fig. 1(b)]. Kambour has reported craze structures of the same dimensions.<sup>17</sup> Annealing below  $T_g$  promotes extreme localization, evident as wider and fewer shear bands in Fig. 1(b), although Fig. 1(a) shows that the quenched APS films can also deform by local shear-band propagation. Where shear bands reach the edge of a craze, discrete steps appear, again emphasizing the localization of the plastic strain. It is likely that the angular orientation of the shear lines in these thin films (about 50° to the tensile direction) is due to the two-dimensional nature of the strain geometry rather than to the effect of the normal-stress component, as is thought to be true in bulk samples.

Figures 2(a) and 2(b) show similar results for a partially crystalline IPS thin film. It is noted that the spherulites in this film tend to break up only after substantial deformation has occurred in the connecting amorphous regions and also that the shear line interspacings are of the order of 200–700 Å [Fig. 2(b)].

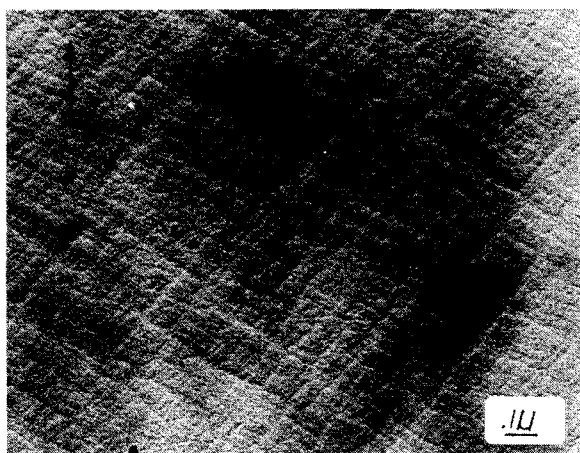
The contrast between quenched and annealed thin films of PMMA is even more dramatic. The quenched and drawn material shown in Fig. 3(a) shows no evidence of localized shear banding, while the well-annealed film in Fig. 3(b) does exhibit both crazing and shear banding, although with reduced intensity when compared to APS. The inset in Fig. 3(b) shows a crazed region which appears to be an arrangement of 200-Å regions rather than continuous 200-Å fibrils.

In bulk materials there is also some evidence for localized shear resulting in a nonuniform surface texture several hundred angstroms in diameter. Figures 4(a) and 4(b) contrast the surface features of APS tensile samples that were ice quenched [Fig. 4(a)] and annealed [Fig. 4(b)] before drawing. The quenched material formed a uniform neck which propagated the length of the sample resulting in the 300–500-Å texture seen in Fig. 4(a). The annealed material whitened, crazed, and fractured even at low strain rates (0.004 min<sup>-1</sup>), resulting in the localized texture of Fig. 4(b) where series of very well-defined surface steps are evident.

Figure 5(a) shows the nonuniform 300–450-Å texture seen on a well-annealed PC surface after necking. Replicas taken from the unstretched material show a rather ill-defined texture of similar dimensions. Figure 5(b) shows that a thin Pt layer deposited prior to deformation breaks up in various places



(a)



(b)

FIG. 2. (a) Pt-C surface replica of partially crystalline isotactic polystyrene thin film drawn 25%. The connecting amorphous regions deform prior to the breakup of the spherulities. (b) A higher magnification of (a) with small arrows indicating interspacings of 200 Å and 500 Å.

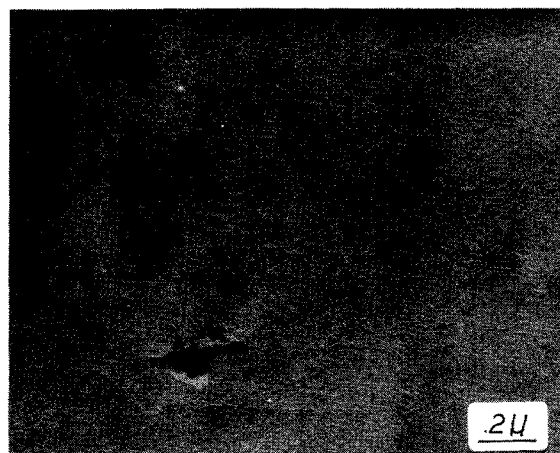
to reveal a texture similar to that seen by direct Pt shadowing, thus reinforcing our assessment of Fig. 5(a).

The surface features of an APS sample deformed in compression at 80 °C and a nominal strain rate of 4 min<sup>-1</sup> are shown in Fig. 6. Sharp shear bands [Fig. 6(a)] initiate at the notch and propagate at an angle of 35°–40° to the compression direction resulting in steps at the back edge of the sample [Fig. 6(b)]. Structural features within the band are 400–1000 Å.

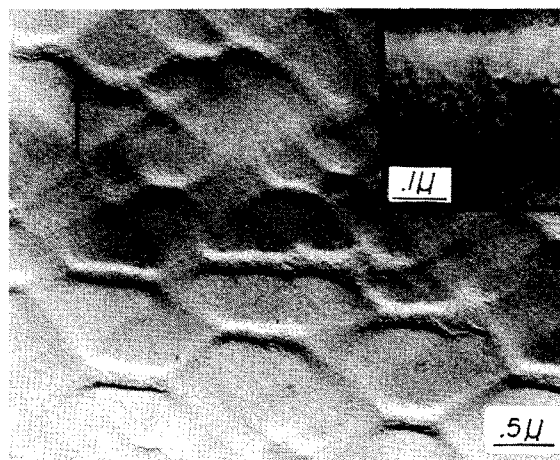
#### Density Measurements

Table I gives the measured densities for PS, PC, and PMMA. Of particular note is the density increase upon annealing for PS and PC, and the den-

sity increase upon plastic deformation for all polymers tested. The maximum density increase upon annealing is small (about +0.04%) but is consistent for PS and PC. PS and PMMA undergo density increases upon hot stretching and even larger increases upon plastic deformation. Maximum increases upon plastic deformation of about 0.25% in PS, 0.25% in PC, and 0.3% in PMMA have been observed. Ender has reported a density increase of about +0.5% in PMMA.<sup>18</sup> The density of compression shear banded material was estimated by noting that the banded region contained approximately 50% deformed material (determined by light microscopy) and then extrapolating from the measured density of the banded region (1.0505) to the density of 100% deformed material (1.0514). It is significant to note that, whether in tension or compression,

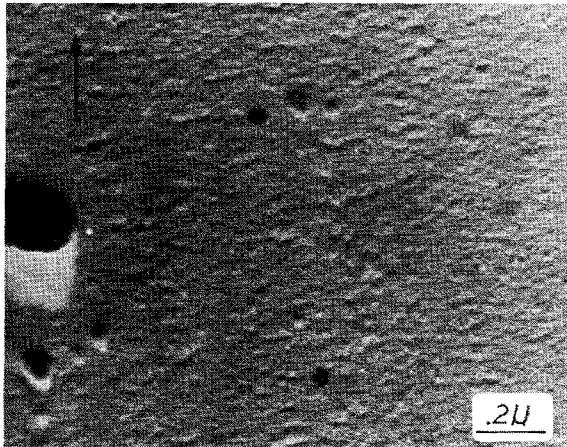


(a)

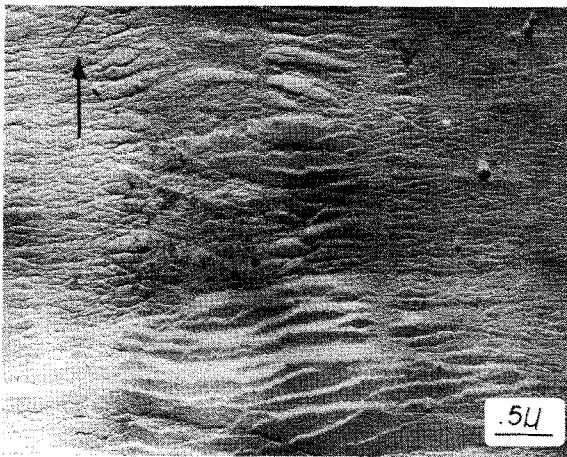


(b)

FIG. 3. (a) Pt-C surface replica of polymethyl methacrylate thin film quenched from 120 °C and drawn 25%. (b) Pt-C surface replica of polymethyl methacrylate thin film annealed for 2 days at 95 °C and drawn 25%. Small arrows in the inset indicate 200-Å regions within the craze.



(a)



(b)

FIG. 4. (a) Pt-C surface replica of bulk atactic polystyrene oriented 5: 1 at 120 °C and quenched before cold drawing at 40 °C showing a 300–450-Å surface texture. (b) Pt-C surface replica of bulk atactic polystyrene oriented 5: 1 at 130 °C, quenched and then reannealed for 6 days at 75 °C before cold drawing at 25 °C. Extreme localization produces numerous surface steps and a texture as small as 200 Å.

plastic deformation densifies the material, albeit not uniformly.

#### Mechanical-Compression Studies

The original derivation<sup>19,20</sup> and subsequent modifications of the "activated flow" model can be found in the literature.<sup>21–24</sup> The model used in this analysis is given by the following exponential expression:

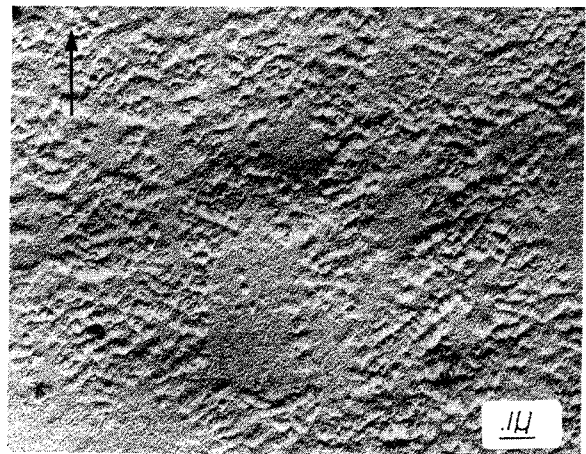
$$\frac{d\epsilon}{dt} = \dot{\epsilon}_0 \exp\left(-\frac{E_0 - \frac{1}{2}\tau_c V_h}{kT}\right), \quad (1)$$

where  $d\epsilon/dt$  is the strain rate,  $\dot{\epsilon}_0$  is the frequency factor,  $k$  is Boltzmann's constant,  $T$  is the temperature,  $E_0$  is the activation energy barrier, and

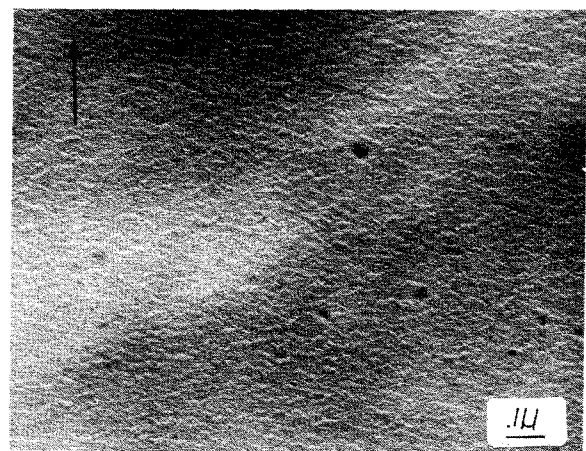
$\frac{1}{2}\tau_c V_h$  is the work done by a critical shear stress  $\tau_c$  to move an elemental shear area  $A$  a distance  $\frac{1}{2}b$  along the shear plane, where  $V_h = Ab$ .

If the normal-stress component acting across the shear plane does not affect the yielding behavior (as is nearly true in metals), then the critical shear stress is equal to the applied shear stress. It has been shown, however, that the large strength differential between compression and tension in polymeric materials is due to the influence of the normal-stress component across the shear plane.<sup>21,25</sup>

The Coulomb-Navier yield criterion,<sup>26</sup> previously shown to be consistent with glassy polymer behavior,<sup>13,21</sup> accounts for this effect by assuming that the intrinsic shear strength of a material is



(a)



(b)

Fig. 5. (a) Pt-C surface replica of polycarbonate cold drawn at 130 °C showing a nonhomogeneous 300–450-Å surface texture. (b) Pt layer deposited on PC before cold drawing at 25 °C showing a 300–450-Å texture as the Pt layer breaks up.

increased by a constant times the normal-stress component across the shear plane:

$$\tau_A = \tau_c - \sigma_A \tan \phi. \quad (2)$$

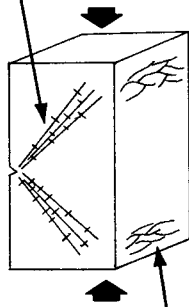
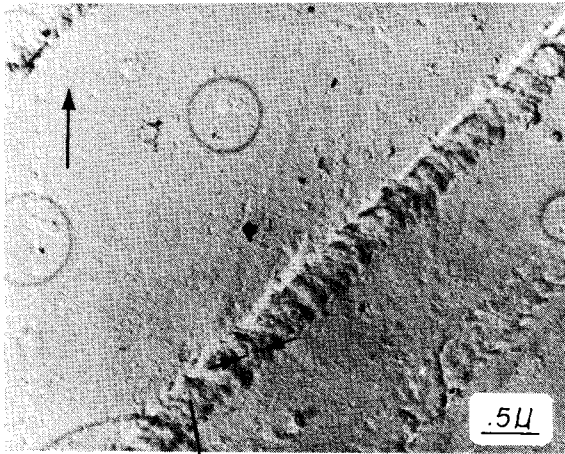


FIG. 6. (a) Pt-C surface replica of compression deformation bands in atactic polystyrene produced at 80°C at a nominal strain rate of 4 min<sup>-1</sup>. Small arrows indicate a 500–1000-Å texture within the bands. (b) Pt-C surface replica of steps produced when deformation bands reach the back edge of the sample. Small arrow points to a step which has caused a slight displacement of the surface polish marks.

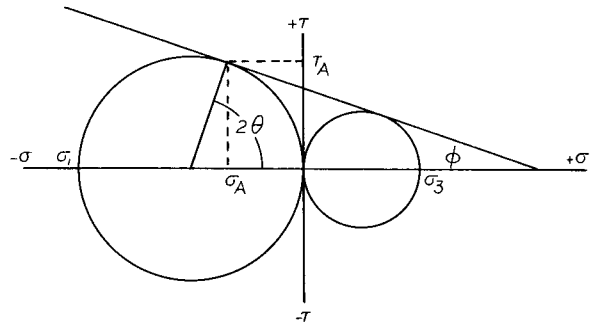


FIG. 7. Typical Mohr circles representing the compressive and tensile yield strengths of a glassy polymer.

In this formulation of the yield criterion  $\tau_c$  is the critical shear stress,  $\tau_A$  is the applied shear stress,  $\sigma_A$  is the applied normal stress across the plane of failure, and  $\tan \phi$  is the coefficient of internal friction, where  $\phi$  is the angle between the normal-stress axis and a tangent drawn to Mohr circles in tension and compression (see Fig. 7). The angle  $\theta$  then is the angle which the plane of failure makes with the compressive axis, and the applied shear and normal stresses across the plane of failure are given geometrically by

$$\begin{aligned} \tau_A &= \frac{1}{2}\sigma_1 \sin\left(\frac{1}{2}\pi - \phi\right), \\ \sigma_A &= \frac{1}{2}\sigma_1 [1 - \cos\left(\frac{1}{2}\pi - \phi\right)], \end{aligned} \quad (3)$$

where  $\sigma_1$  is the applied compressive stress. Substitution of Eqs. (2) and (3) into Eq. (1) gives

$$\begin{aligned} \frac{d\epsilon}{dt} = \dot{\epsilon}_0 \exp & - \left\langle \frac{E_0}{kT} - \frac{\frac{1}{2}\sigma_1 V_h}{2kT} \left\{ \sin\left(\frac{1}{2}\pi - \phi\right) \right. \right. \\ & \left. \left. - [1 - \cos\left(\frac{1}{2}\pi - \phi\right) \tan \phi] \right\} \right\rangle, \end{aligned} \quad (4)$$

where the critical shear stress has been corrected for the effect of the normal-stress component across the shear plane.  $V_h$  can be calculated by taking the slope of the  $\ln(d\epsilon/dt)$ -vs- $\sigma_1$  plot and applying Eq. (4).  $E_0$  is found from the displacement of these curves with respect to temperature.

We have found the angle  $\phi$  experimentally for both PC and APS by comparing tensile and compressive data as is demonstrated in Fig. 7. Our results show  $\phi = 7.5^\circ$  for PC and  $\phi = 10^\circ$  for APS which compare favorably with Whitney's experimental value of  $13^\circ$  for APS.<sup>21</sup> By extrapolating from data by Sternstein *et al.*,<sup>27</sup> which compared shear and tensile yield stress values for PMMA, we have assumed a value of  $\phi = 10^\circ$  for the analysis of our PMMA data.

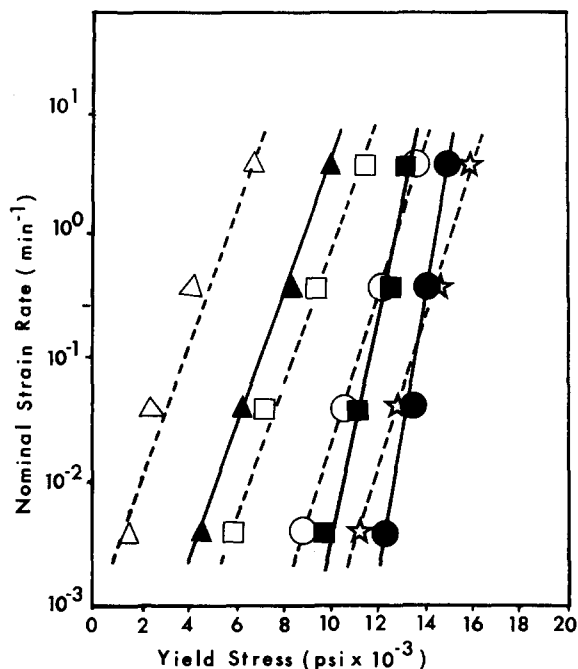


FIG. 8. Strain-rate dependence of the yield stress for APS ice quenched from 105°C through  $T_g$ :  $\Delta$  80°C,  $\square$  60°C,  $\circ$  40°C,  $\star$  24°C; for APS ice quenched from 105°C and reannealed 6 days at 75°C:  $\blacktriangle$  80°C,  $\blacksquare$  60°C,  $\bullet$  40°C.

The  $\ln$  of the nominal strain rate is a linear function of yield stress for both PS and PC, but the relationship is nonlinear for PMMA. The nonlinear relationship found for PMMA is in agreement with tensile data reported by Roetling<sup>11</sup> for this range of strain rates, while Holt<sup>12</sup> found a straight line relationship in compression. Figure 8 shows an example of our stress-strain rate data for APS.

Of all the thermal histories applied to each of the four polymers, only rapid quenching from the melt produced significant deviations in the stress-strain behavior. Slow cooling from the melt or annealing just below  $T_g$  produced nearly identical behavior for both PS and PC while ice quenching produced significantly lower yield stresses and decreased the slope of the  $\ln(\text{strain rate})$ -vs.-yield stress plots. Ice quenching also lowered the yield stresses for PMMA but did not affect the slope of the  $\ln(\text{strain rate})$ -vs.-yield stress plots.

Table II presents the values for "activation energy" and "shear activation volume" as calculated from our data by the above procedure. Figure 9 gives the activation volumes as a function of test temperature for PC and PS but not for PMMA in which  $V_h$  also varied as a function of strain rate. A distinction is made in Table II between quenching and annealing for PS and PC but not for PMMA, since

no variation in either  $V_h$  or  $E_0$  was observed for this material as a function of thermal history (at least in the temperature range investigated).

Values for annealed PS and annealed PC represent averages of three separate thermal histories which involved annealing, and the values for PMMA represent averages for all four thermal histories. Only the PS data were extensive enough to allow calculation of  $V_h$  and  $E_0$  for values of  $T > T_g$ , and for this material there appear to be rather abrupt changes in the values of these parameters at  $T = T_g$ . The same change might be expected for PC at around 145°C. Values for PMMA are listed for two different strain rates and four different temperatures to demonstrate the large changes (compared to PS and PC) that occur in these parameters when either strain rate or temperature is varied. This behavior for PMMA is not unexpected since the reported  $\beta$  transition occurs at about 45°C,<sup>28</sup> while no major transitions occur for PS and PC within the temperature ranges investigated.

#### DISCUSSION

In well-annealed glassy polymers yielding and subsequent plastic deformation are evidenced by localized shear displacements occurring at 100–1000-Å interspacings. This ability to undergo local deformation at regular interspacings implies a microstructure that is not homogeneous, one in which adjacent regions can move relative to one another for short distances. Whether or not these spacings, observable in both crazing and shear yielding, result directly from the presence of ordered regions requires further study, but there is evidence for microstructural movement as opposed to uniform deformation which one might expect if the glassy state assumes an "homogeneous" random coil-type chain conformation.

The density increase upon annealing is small but consistent for APS and PC and must represent an ordering process which results in increased strength and an increased propensity for localized deformation. Plastic deformation produces a further density increase that is probably localized, at least in those materials where the plastic strain is limited to narrow bands.

An Eyring-type flow model has been employed in an effort to make a physical estimate of the quantity of material moving at the yield point. There is not yet sufficient evidence for a true physical interpretation of  $V_h$ , but several related observations may be made. The increase in  $V_h$  of annealed PS and PC is consistent with the measured density increase in annealed samples, suggesting that the size of the flow unit is somehow related to the ordering effects of annealing. It is also interesting

TABLE II. Calculated values for "shear activation volume" and "activation energy".

Polymer	Thermal history	Strain rate (min <sup>-1</sup> )	Test temp range (°C)	V <sub>h</sub> <sup>a</sup> Shear activation volume (Å <sup>3</sup> )	E <sub>0</sub> <sup>a</sup> Activation energy barrier (kcal/mole)
APS (T <sub>g</sub> ≈ 75 °C)	ice quenched from T(105°C) > T <sub>g</sub> well annealed at T = 75 °C	...	25 < T < 75	3890	39.9
		...	75 < T < 90	3440	102.5
IPS (T <sub>g</sub> ≈ 100 °C) (T <sub>m</sub> ≈ 250 °C)	ice quenched from T(260 °C) > T <sub>m</sub> (amorphous)	...	25 < T < 75	6300	59.9
		...	75 < T < 90	4330	104.6
IPS (T <sub>g</sub> ≈ 100 °C) (T <sub>m</sub> ≈ 250 °C)	ice quenched from T(260 °C) > T <sub>m</sub> annealed 1 hr at 180 °C (crystalline)	...	25 < T < 75	3730	47.1
		...	25 < T < 75	3200	43.4
PC (T <sub>g</sub> ≈ 145 °C) (T <sub>m</sub> ≈ 250 °C)	ice quenched from T(260 °C) > T <sub>m</sub> well annealed at T = 145 °C	...	25 < T < 100	11770	73.9
		...	25 < T < 100	14580	86.6
PMMA (T <sub>g</sub> ≈ 100 °C)	all thermal histories	10 <sup>1</sup>	26	1310	39.0
			40	1390	35.2
			60	1650	36.3
			80	1990	41.9
		10 <sup>-1</sup>	26	3590	74.9
			40	3840	64.4
			60	4980	80.3
			80	5860	78.6

<sup>a</sup>Experimental error estimated to be ±15%.

to note the similar V<sub>h</sub> values for APS and crystalline IPS, suggesting that even in crystalline IPS (about 20% crystallinity as judged from density) the deformation is occurring in the connecting amor-

phous regions. This observation is supported by the thin-film experiments (Fig. 2) where deformation of the amorphous regions precedes the breakup of the spherulites. Our results on PS and PC

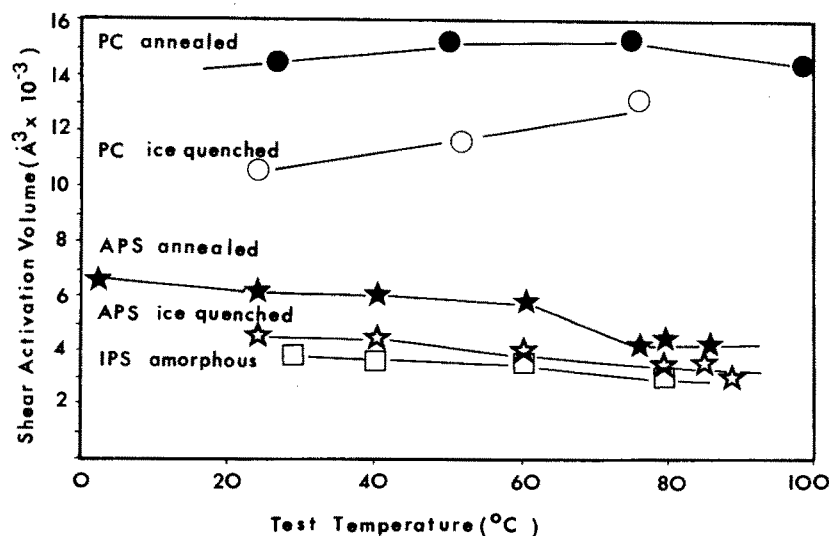


FIG. 9. Average activation volume parameter vs test temperature for ○ PC ice quenched from 260 °C through T<sub>m</sub>, ● PC annealed at 145 °C; ☆ APS ice quenched from 105 °C through T<sub>g</sub>, ★ APS annealed at 75 °C, and □ IPS quenched from 260 °C (amorphous).



seem to be consistent with an activated flow model where  $V_h$  is essentially constant for test temperatures up to  $T_g$ , while the variation of  $V_h$  with both temperature and strain rate for PMMA is more difficult to interpret, although the occurrence of the secondary transition at about 45°C may contribute to these effects.

The activation energies for yielding appear to increase for increasing temperatures, approaching values of about 100 kcal/mole near  $T_g$ . These values (~100 kcal) are very close to values for the  $T_g(\alpha)$  transitions in both PS, PC, and PMMA as reported by Boyer.<sup>28</sup> However, below  $T_g$ , the activation energies for yielding have values which are generally above the reported values<sup>28</sup> for the  $\beta$  transitions in these polymers, and they also appear to be somewhat dependent upon thermal history and temperature. These observations suggest that the yielding process below  $T_g$  cannot be directly attributable to a unique relaxational transition or associated with only one type of molecular motion.

#### CONCLUSIONS

Glassy polymers exhibit intense localized yielding modes when well annealed just below the glass transition temperature. Rapid cooling from the melt results in both lower density and the tendency to deform homogeneously. Localized yielding manifests itself as shear displacements occurring at 100–1000-Å interspacings which result in surface steps at the sample edge. The yielding process below  $T_g$  does not appear to be attributable to a unique relaxational transition and hence cannot be associated with a unique molecular motion.

#### ACKNOWLEDGMENT

The authors wish to thank the Whirlpool Corporation for partial support of this study.

<sup>1</sup>G. S. Y. Yeh, *J. Macromol. Sci.* (to be published).

<sup>2</sup>G. S. Y. Yeh and P. H. Geil, *J. Macromol. Sci. (Phys.)* 1, 235 (1967).

<sup>3</sup>S. H. Carr, P. H. Geil, and E. Baer, *J. Macromol. Sci. (Phys.)* 2, 13 (1968).

<sup>4</sup>T. G. F. Schoon and O. Teichmann, *Kolloid-Z* 197, 35 (1964).

<sup>5</sup>K. H. Yang and J. L. Kardos, American Physical Society, Division of High Polymer Physics Meeting, Cleveland, Ohio, 1971 (unpublished).

<sup>6</sup>D. Luch and G. S. Y. Yeh, American Physical Society, Division of High Polymer Physics Meeting, Cleveland, Ohio, 1971 (unpublished).

<sup>7</sup>P. Zitek and J. Zelinger, *J. Appl. Polymer Sci.* 44, 1213 (1970).

<sup>8</sup>C. Bauwens-Crowet, J. C. Bauwens, and G. Homes, *J. Polymer Sci.* 7, 735 (1969).

<sup>9</sup>C. Crowet and G. A. Homes, *Appl. Mater. Res.* 3, 1 (1964).

<sup>10</sup>J. J. Lohr, *Trans. Soc. Rheol.* 9, 65 (1965).

<sup>11</sup>J. A. Roetling, *Polymer* 6, 311 (1965).

<sup>12</sup>D. H. Holt, *J. Appl. Polymer Sci.* 12, 1653 (1968).

<sup>13</sup>R. N. Hayward, B. M. Murphy, and E. F. T. White, *J. Polymer Sci. Part A-2* 9, 801 (1971).

<sup>14</sup>P. B. Bowden and S. Raha, *Phil. Mag.* 22, 463 (1970).

<sup>15</sup>P. B. Bowden, *Phil. Mag.* 22, 455 (1970).

<sup>16</sup>*ASTM Standards, No. 27, test D 1505* (American Society for Testing and Materials, Philadelphia, Pa., 1967).

<sup>17</sup>R. P. Kambour and A. S. Holik, *J. Polymer Sci. Part A-2* 7, 1393 (1969).

<sup>18</sup>D. H. Ender, *Polymer Preprints, ACS* (New York) 10, 1132 (1969).

<sup>19</sup>H. Eyring, *J. Chem. Phys.* 3, 107 (1935).

<sup>20</sup>H. Eyring, *J. Chem. Phys.* 4, 283 (1936).

<sup>21</sup>W. Whitney, Sc. D. thesis (MIT, 1964) (unpublished).

<sup>22</sup>E. J. Kramer, *J. Appl. Polymer Sci.* 14, 2825 (1970).

<sup>23</sup>J. S. Lazurkin, *J. Polymer Sci.* 30, 595 (1958).

<sup>24</sup>R. E. Robertson, *J. Appl. Polymer Sci.* 7, 443 (1963).

<sup>25</sup>J. C. Bauwens, *J. Polymer Sci. Part A-2* 8, 893 (1970).

<sup>26</sup>J. C. Jaeger, *Elasticity, Plasticity, and Flow* (Wiley, New York, 1962).

<sup>27</sup>S. S. Sternstein, L. Ongchin, and A. Silverman, *Appl. Polymer Symp.* 7, 175 (1968).

<sup>28</sup>R. F. Boyer, *Rubber Rev.* 36, 1303 (1963).